Astronomy Reports, Vol. 43, No. 10, 1999, pp. 631–636. Translated from Astronomicheskii Zhurnal, Vol. 76, No. 10, 1999, pp. 723–728.
Original Russian Text Copyright © 1999 by Botashev, Gorshkov, Konnikova, Mingaliev.

Multifrequency Spectra of a Complete Sample of Radio Sources with Steep Spectra (< –0.5)

A. M. Botashev[1], A. G. Gorshkov[2], V. K. Konnikova[2], and M. G. Mingaliev[1]

[1]*Special Astrophysical Observatory, Russian Academy of Sciences, Nizhnii Arkhyz, Karachaevo-Cherkesskaya Republic, 357147 Russia*

[2]*Sternberg Astronomical Institute, Universitetskii pr. 13, Moscow, 119899 Russia*

Received April 20, 1998

Abstract—The observations of a complete sample of radio sources with spectral indices $\alpha < -0.5$ ($S \propto \nu^{\alpha}$) are presented. The sample was selected from the Zelenchuk Survey at 3.9 GHz, and contains all sources in the declination range 4°–6° at Galactic latitudes $|b| > 10°$ with 3.9-GHz fluxes exceeding 200 mJy. Accurate flux densities of the sample sources were measured at 0.97, 2.3, 3.9, 7.7, 11.2, and 21.7 GHz. For some of the objects, angular sizes and degrees of polarization are estimated. The spectra of the sample sources in the frequency range from 0.365–21.7 GHz are studied.

1. INTRODUCTION

Radio sources with steep spectra ($\alpha < -0.5$, $S \propto \nu^{\alpha}$) are objects in which the dominant contribution to the observed emission is made by extended structures with typical sizes of hundreds of kiloparsecs and larger. As a rule, the emission of the compact cores, which dominates in flat-spectrum sources, is negligible in these objects. Therefore, the emission of these sources is constant over long timescales, comparable to or greater than the entire history of radio astronomy.

Studies of these sources over a wide frequency range make it possible to explore in detail their spectral characteristics and to obtain answers to a number of questions, in particular, how closely the emission follows a power law. Deviation from a power law at high frequencies indicates an appreciable contribution of compact structures to the total emission, and the low-frequency cutoff is determined by the angular sizes of the extended structures. In this work, we studied a complete sample; therefore, our results give a realistic idea about the classification of the spectral characteristics and, hence, the morphology of steep-spectrum sources.

The sample considered was selected from the Zelenchuk Survey at 3.9 GHz [1], and contains all sources in the declination range 4°–6° at Galactic latitudes $|b| > 10°$ with 3.9-GHz fluxes greater than 200 mJy. A complete list of sample sources and measurements made at particular epochs were published in [2–4].

Here, we present the spectra of the sample sources with spectral indices $\alpha < -0.5$, obtained from observations on the RATAN-600 radio telescope at 0.97, 2.3, 3.9, 7.7, 11.2, and 21.7 GHz.

2. OBSERVATIONS AND EQUIPMENT

The observations were carried out in 1996–1997 on the Northern (azimuth 0°) and Western (azimuth 270°) sectors of the RATAN-600 radio telescope using the transit method in a fixed-focus regime [5]. All sources were observed in series of 15–30 days, on average, three times per year.

The initial coordinates of the sample sources from the Zelenchuk Survey have large errors in declination; therefore, for most sources, we used coordinates obtained from VLA measurements [6], the Texas Survey [7] (improved in [8]), and the NVSS Survey, as well as from our own observations. We obtained the NVSS coordinates from the database of the Special Astrophysical Observatory [9].

The parameters of the receivers used on the Northern sector of the RATAN-600 telescope are given in [10, 11].

The parameters of the antenna beam for observations at the meridian and azimuth 270° are substantially different. In observations on the Northern sector, the beamwidth varies in right ascension from 11″ to 235″ and in declination from 1′.4 to 30′ from 21.7 to 0.97 GHz. The beamwidth for the Western sector varies in right ascension from 18″.5 to 412″ and in declination from 7′.8 to 172′ at the same frequencies. At 21.7, 11.2, and 7.7 GHz, where beam switching is used, the separations between the beams are 0.54′, 1.82′, and 3.8′ on the Northern sector and 0.92′, 3.24′, and 6.9′ on the Western sector, respectively.

The polarization electric vector coincides with the vertical for all receivers except the 3.9-GHz receiver, for which it is 90° from the vertical.

The position angles of transit of a source through the beam are quite different (by approximately 45°) for

1063-7729/99/4310-0631$15.00 © 1999 å Äà ä “ç ‡Ûí‡/Interperiodica”

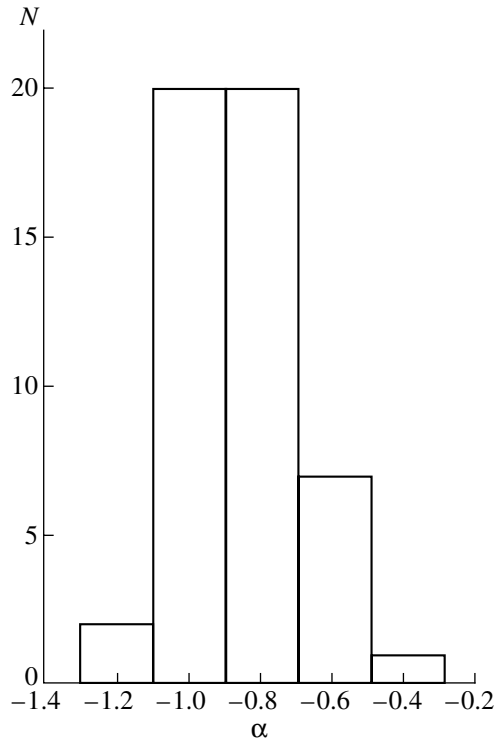

Distribution of spectral indices for sources with power-law spectra.

observations at azimuths of 0° and 270°; therefore, for sources with appreciable linear polarization, the flux densities observed in the two azimuths should be different. Accordingly, with precise measurements, we can detect the presence of linear polarization in such sources.

3. CALIBRATION

In the fixed-focus regime, the range of possible elevations of radio sources is restricted; therefore, we used for calibration the strongest source in the sample, 2128+048. This source is unresolved at 21.7 GHz, the highest frequency for our observations. We adopted flux densities for 2128+048 at 0.97, 2.3, 3.9, 7.7, 11.1, and 21.7 GHz of 4.25, 3.07, 2.35, 1.57, 1.24, and 0.75 Jy, respectively. The adopted flux scale coincides with that of the MGB Surveys at 1.4 and 4.85 GHz.

4. DATA PROCESSING AND FLUX ERRORS

To process the observations, we created a software package enabling us to derive fluxes for each observation of a source, as well as mean fluxes for one or several observation cycles. Optimal filtering of the input data forms the basis for the reduction; the procedure is described in detail in [12]. Prior to filtering, nonlinear filters were used to clean the input data of pulse interference, jumps, and trends with timescales longer than the scale of the telescope beam. When deriving the mean fluxes, we used only those records for which the noise dispersion belonged to one general group; the procedure for selecting such records is described in [13].

The mean fluxes were determined using two methods: as the weighted-mean value $\hat{S}$ of the fluxes measured in each observation, and as the flux obtained via optimal filtering of the summed, cleaned input records. When summing, we used nonlinear filtering; this reduces the weight of poor records. It is clear that the fluxes obtained using these two methods should be similar, and a significant difference testifies to the presence of a bad record that has not been eliminated by preliminary filtering. We also determined the errors using two methods:

$$\sigma_s = \left(\left(\sum_i^n (S_i - \hat{S})^2\right)/n(n-1)\right)^{1/2},$$

where S_i is the flux for the ith observation, $\hat{S}$ is the weighted-mean flux, n is the number of observations, and

$$\sigma_{ii} = \left(\sigma^2/\sum_i A_i^2\right)^{1/2},$$

where σ^2 is the dispersion of the sum of the residual noise of all the records after elimination of the source signal, and A_i are tabulated values of the telescope beam.

If there is no non-noiselike signal in the records, the two error estimates should be close to each other. In reality, as a rule, the error σ_s is larger, indicating the presence of a determinate signal in the noise; in the case of large differences, additional searches for and elimination of poor records is required. In any case, we adopted the larger of the two values as the error of the measured flux. For low signal-to-noise ratios, when the source was not detected in each record, we applied only the second method for flux measurement and error estimation. For steep-spectrum sources, this is usually the situation at 21.7 GHz.

The processing procedure used is not optimal for sources with angular sizes that are comparable to the beam size; therefore, the fluxes of extended sources may be underestimated at one or several frequencies.

For sources with known linear polarization, we used the fluxes obtained using the formula [14]

$$S = 0.5S_0[1 + p\cos 2(q - \chi - \psi)],$$

where S_0 is the total emitted flux density of the source, p and q are the degree of linear polarization and the parallactic angle, χ is the angle between the plane of linear polarization and the vertical, and ψ is the polarization position angle.

Approximation of the source spectra

Name	R. A.	Dec		*A*	*B*	*C*
0004+053*	$00^h04^m32^s.54$	05°19′27″99	S	2.973	–0.870	
0011+054	00 11 27.44	05 28 30.42	C_-	3.254	–0.888	–0.103
0020+042	00 20 45.75	04 12 17.84	S	2.881	–0.893	
0037+046*	00 37 17.25	04 39 03.37	S	3.028	–0.906	
0059+056	00 59 36.57	05 39 06.20	C_-	2.959	–0.736	–0.057
0100+050	01 00 53.60	05 05 25.49	S	2.850	–0.849	
0127+057*	01 27 26.95	05 47 33.51	S	2.735	–0.742	
0208+040	02 08 08.09	04 05 27.97	C_-	3.002	–0.461	–0.402
0210+055	02 10 58.81	05 33 48.34	S	2.955	–1.002	
0248+059*	02 48 24.36	05 59 45.26	S	3.132	–0.943	
0253+041	02 53 18.26	04 07 34.91	S	2.749	–0.603	
0309+040	03 09 25.90	04 02 56.96	S	2.808	–0.978	
0311+057	03 11 15.48	05 46 54.28	S	2.740	–0.786	
0320+053	03 20 41.52	05 23 33.78	C_-	3.544	–0.788	–0.133
0340+048*	03 40 51.52	04 48 22.25	S	3.578	–0.914	
0347+057*	03 47 07.08	05 42 32.18	S	3.601	–0.715	
0359+055*	03 59 29.40	05 32 54.35	S	2.958	–0.977	
0411+055	04 11 58.17	05 27 13.20	C_-	3.345	–0.500	–0.119
0423+047*	04 23 40.08	04 43 41.41				
0432+044	04 32 33.81	04 27 49.70	S	3.123	–0.831	
0441+056	04 41 58.88	05 40 42.36	C_-	2.929	–0.404	–0.235
0511+053	05 11 27.04	05 22 18.17	C_-	2.958	–0.543	–0.141
0530+040*	05 30 25.30	04 03 51.84	S	3.355	–0.696	
0531+050*	05 31 55.62	05 01 43.74				
0534+041	05 34 42.83	04 11 59.12	S	2.810	–0.843	
0558+052	05 58 44.98	05 13 03.77	S	2.716	–0.736	
0719+056*	07 19 02.87	05 37 10.84	S	3.010	–0.598	
0740+052*	07 40 00.11	05 14 12.44	C_-	2.900	–0.571	–0.216
0756+040	07 56 04.00	04 02 52.93	S	2.792	–0.809	
0806+059	08 06 04.02	05 59 24.05	C_+	2.805	–0.831	0.304
0808+044	08 08 27.53	04 29 18.37	C_-	2.995	–0.675	–0.192
0833+042	08 33 23.73	04 17 03.13	C_-	2.684	–0.495	–0.163
0905+044	09 05 13.43	04 25 35.23	S	2.933	–0.940	
0911+048	09 11 09.74	04 48 56.80	C_-	2.661	–0.248	–0.430
0944+045	09 44 05.75	04 32 54.30	S	2.883	–0.920	
0944+059	09 44 32.27	05 56 19.59	S	3.042	–1.089	
1017+040	10 17 58.35	04 05 57.99	C_+	2.952	–1.069	0.263
1028+049*	10 28 43.10	04 58 35.10				
1057+050	10 57 36.20	05 00 07.93	C_-	2.794	–0.645	–0.169
1104+058	11 04 40.56	05 49 24.66	C_+	2.858	–1.159	0.325
1107+045	11 07 35.58	04 34 00.45	S	2.999	–1.138	
1120+057	11 20 34.30	05 46 47.75	S	3.353	–0.999	
1122+052*	11 22 03.83	05 12 57.37	S	3.112	–0.846	
1129+052*	11 29 21.86	05 12 22.70	S	2.829	–0.773	
1146+052	11 46 12.38	05 12 06.50	S	3.034	–1.264	
1152+046	11 52 19.50	04 40 54.61	S	3.031	–0.984	
1200+045	12 00 48.16	04 31 00.25	S	3.105	–0.479	
1203+043	12 03 46.21	04 22 53.01	S	3.325	–0.993	
1236+055*	12 36 36.29	05 35 46.37	S	3.090	–0.998	
1309+041	13 09 49.98	04 09 41.22	S	2.868	–0.773	
1338+044	13 38 50.15	04 29 32.07	S	2.958	–1.019	
1340+053	13 40 12.44	05 19 36.99	C_+	3.323	–0.745	0.176
1349+048	13 49 06.30	04 50 29.31	C_-	2.941	–0.567	–0.207
1423+046	14 23 58.27	04 40 24.88	S	2.755	–0.717	
1434+036	14 34 25.94	03 37 11.17	S	3.500	–0.567	
1436+046	14 36 34.09	04 41 21.45	S	2.812	–0.761	
1443+044*	14 43 38.40	04 25 18.22				

Table. (Contd)

Name	R. A.	Dec		*A*	*B*	*C*
1451+041	14 51 07.92	04 11 45.07	S	2.681	–0.684	
1520+041	15 20 02.66	04 11 09.47	S	3.010	–0.962	
1553+045	15 53 08.73	04 35 53.95	S	2.873	–0.796	
1611+042*	16 11 44.93	04 13 23.89	S	3.139	–0.935	
1617+043	16 17 38.50	04 24 34.40	S	2.744	–0.668	
1652+040	16 52 58.73	04 00 53.34	C_+	2.832	–0.670	0.098
1703+051*	17 03 58.76	05 06 37.14				
1719+047	17 19 45.74	04 46 06.22	S	2.984	–0.947	
1734+056	17 34 49.75	05 39 14.41	S	2.851	–1.059	
1751+050	17 51 49.47	05 00 08.88	C_-	3.014	–0.492	–0.105
1753+049	17 53 23.03	04 55 17.01	C_+	2.713	–0.716	0.137
1810+046*	18 10 47.56	04 38 39.93	S	3.435	–0.802	
1933+058*	19 33 17.66	05 50 00.66				
1939+055	19 39 55.80	05 31 20.81	C_-	2.830	–0.831	–0.048
1955+041	19 55 07.83	04 08 35.89	S	2.767	–0.694	
2042+045	20 42 15.67	04 33 09.83	S	2.933	–0.844	
2055+055	20 55 59.79	05 31 10.98	C_-	3.155	–0.766	–0.143
2115+056	21 15 10.86	05 39 36.83	C_-	2.733	–0.405	–0.235
2142+042*	21 42 46.85	04 17 41.29	C_-	3.171	–0.453	–0.261
2150+053	21 50 54.30	05 22 08.78	S	3.172	–0.866	
2159+043	21 59 28.91	04 20 49.39	S	3.300	–0.745	
2203+056	22 03 50.36	05 41 33.20	C_-	3.095	–0.614	–0.118
2222+051*	22 22 43.43	05 11 53.85	S	3.071	–0.944	
2338+042	23 38 24.67	04 14 37.06	C_+	3.327	–1.021	0.081
2350+057	23 50 21.12	05 43 50.97	S	3.183	–1.000	

Note: 0004+053. At 0.97 and 2.3 GHz, a nearby source falls in the beam.
0037+046. The source is double, with the separation between the components being 16.″9 and the components' flux ratio 1 : 0.65 [6]. The flux densities are underestimated above 7.7 GHz.
0127+057. At 0.97 GHz, a nearby source falls in the beam.
0248+059. The source is polarized; at 11 cm, $p = 7.9\%$, PA = 36° [16]. The angular size is 15″–20″. The flux densities are underestimated above 7.7 GHz.
0340+048. The source is extended, with a 4″ core and 17″ halo [17]. The flux densities are underestimated above 11.2 GHz.
0347+057. The source is double, with the separation between the components being $\Delta\alpha = 10''$, $\Delta\delta = 1'$. The flux densities are given for azimuth 0°, where the source is unresolved [18].
0359+055. The source is double, with the separation between the components being 14.″8 and the components' flux ratio 1 : 0.55 [6]. The flux densities are given for azimuth 270°, where the components are not resolved.
0423+047. The source has an extended structure larger than 30″. The flux densities are underestimated above 3.9 GHz.
0530+040. The source is linearly polarized; at 6 cm, $p = 5\%$, PA = 172° [17].
0531+050. The source has an extended structure larger than 20″. The flux densities are underestimated above 7.7 GHz.
0719+056. The source is linearly polarized; at 2.3–7.7 GHz, $p > 7\%$.
0740+052. The source is linearly polarized; at 2.3–7.7 GHz, $p \geq 5\%$. The source is extended, about 20″. The flux densities are underestimated above 7.7 GHz.
1028+049. The source is extended, and the E–W size is 20″. The flux densities are underestimated above 3.9 GHz.
1122+052. The flux density is overestimated at 0.97 GHz, as another source falls in the beam.
1129+052. The source is extended, with a size of about 15″. The flux densities are underestimated above 11.2 GHz.
1152+046. At frequencies of 0.97 and 2.3 GHz, a nearby source falls in the beam.
1236+055. The source is double, with the separation between the components being 55″. The flux densities were obtained in azimuth 270°.
1423+046. The source is triple, 14″ in size [6]. The flux density is underestimated at 21.7 GHz.
1443+044. The source is probably polarized; at 2.3–7.7 GHz, $p > 5\%$. The data are only poorly approximated.
1611+042. The source has an extended structure >15″ in size. The flux densities are underestimated above 7.7 GHz.
1703+051. The source is double, with an E–W size of 2.″3 and a N–S size of 4″. The beam contains both sources at low frequencies and only one source at high frequencies.
1810+046. The source is linearly polarized; at 11.1 cm, $p = 8\%$, PA = 41° [17].
1933+058. The source has an extended structure >15″ in size. The flux densities are underestimated above 7.7 GHz. At 0.97 GHz, a nearby source falls in the beam.
2142+042. The source is double, with an E–W size of about 14″. The flux densities are underestimated above 11.2 GHz.
2222+051. The source is linearly polarized, with $p = 7$–8%.

5. SPECTRA OF THE SAMPLE SOURCES

The sample contains 92 steep-spectrum sources. The source 2128+048 was used to calibrate the flux scale. For nine sources, we could not obtain reliable spectra; some of these are resolved in right ascension at all observation frequencies, and the remaining are blended with other sources nearby in declination. These are 0127+053, 0153+053, 0255+058 (3C 75), 1446+042, 1446+043, 1518+046, 1518+045, 1648+050 (3C 348), and 2310+050 (3C 458.0); they were excluded from the sample.

The weighted-mean fluxes and their rms errors at 0.97, 2.3, 3.9, 7.7, 11.2, and 21.7 GHz were published in [15]. When approximating the flux densities, it is important to exclude flux densities that substantially decrease due to comparable angular sizes of the source and the antenna beam in right ascension.

Thirty percent of the sample sources have angular sizes larger than 10″. The angular sizes of some sources were known earlier; for the remaining sources with angular sizes larger than 15″, we obtained estimates from our observations. Flux densities underestimated due to comparable angular sizes of the source and beam were excluded.

At 21.7 GHz, source angular sizes of 5″–10″ are comparable to the antenna beamwidth in right ascension. Since there is virtually no information on the sample sources with angular sizes smaller than 10″, we fitted their spectra without the 21.7 GHz measurements. A comparison of the approximated and measured flux densities can yield information about the angular sizes of the sources. The flux densities of six sources were underestimated at frequencies above 3.9 GHz due to their angular sizes; we did not approximate their spectra.

Allowing for the flux-density errors, the spectra of 50 sources are well fitted with a logarithmic straight line in the range 0.97–11.2 GHz (S spectra)

$$\log S = A + \alpha \log \nu.$$

The mean value of the spectral index for these sources is -0.857 ± 0.13, which coincides with the mean index obtained for the sample as a whole between 3.9 and 7.5 GHz [4]. The 21.7-GHz fluxes of unresolved sources form an extension of their power-law spectra. The figure shows the distribution of spectral indices for sources with normal spectra.

Taking into consideration the Texas Survey data at 0.365 GHz [7] indicates that, of the 50 sources with power-law spectra in the frequency range considered, only seven are self-absorbed below 0.97 GHz. The spectra of the remaining sources do not deviate from a power law at frequencies from 0.365 to 21.7 GHz.

The spectra of 19 sources flatten toward low frequencies (due to synchrotron self-absorption, C_- spectra), and the spectra of seven sources flatten above 3.9 GHz (C_+ spectra). These spectra are well fitted with a logarithmic parabola:

$$\log S = A + B \log \nu + C \log^2 \nu.$$

Of the 19 self absorbed sources, only two have flux peaks between 0.365 and 0.97 GHz; the spectra of the rest continue to grow over the entire frequency interval considered. Flattening of the spectra above 3.9 GHz is most likely due to the presence of appreciable emission from a compact component.

The table lists the coefficients A, B, and C for our approximations of the spectra, together with the epoch-1950.0 source positions. We provide information about the sources marked with an asterisk in the notes to the table.

Seven sources display linear polarization greater than 5%. For the three sources in which linear polarization is detected in our observations, approximate estimates of the degree of polarization are given in the notes to the table.

6. CONCLUSION

Our study of the spectra of a complete sample of radio sources with steep spectra ($\alpha < -0.5$) in the frequency range 0.97–21.7 GHz has yielded the following results.

(1) The spectra of most of the sources (61%) are well fitted by a logarithmic straight line. Virtually all these sources show no deviation from a power-law spectrum to frequencies as low as 0.365 GHz. The mean spectral index of these sources is -0.857 ± 0.13.

(2) The spectra of 7% of the sources cannot be accurately approximated because their fluxes are underestimated above 3.9 GHz, due to the fact that the source and antenna beam have comparable angular sizes. However, it is very probable that their spectra are also power-law.

(3) The spectra of 23% of the sources are of type C_-, with a flattening in the low-frequency part of the spectrum due to synchrotron self-absorption.

(4) The spectra of 9% of the sources are of type C_+, with a flattening at frequencies above 3.9 GHz; this may be due to the presence of an appreciable compact component in these sources.

(5) Eight percent of the sources have linear polarizations exceeding 5%.

(6) The angular sizes of 30% of the sample sources exceed 10″.

Thus, we have established that the high-frequency spectra of an overwhelming majority of the sample sources are well described by a power law. This provides evidence that either there are no compact components in these sources, or their emission does not exceed a few percent of the emission of the extended (steep-spectrum) component.

REFERENCES

1. Amirkhanyan, V.R., Gorshkov, A.G., Kapustkin, A.A., *et al.*, *Katalog radioistochnikov Zelenchukskogo obzora neba v diapazone sklonenii 0°–14°* (Catalogue of Radio

Sources from the Zelenchuk Survey at Declinations 0°–14°), Moscow: Moscow State University, 1989.
2. Konnikova, V.K. and Sidorenkov, V.N., *Astron. Zh.*, 1988, vol. 65, p. 263.
3. Amirkhanyan, V.R., Gorshkov, A.G., and Konnikova, V.K., *Pis'ma Astron. Zh.*, 1989, vol. 15, p. 876.
4. Amirkhanyan, V.R. and Gorshkov, A.G., and Konnikova V.K, *Pis'ma Astron. Zh.*, 1992, vol. 69, p. 225.
5. Soboleva, N.S., Temirova, A.V., and Pyatunina, T.V., *Preprint of Spetsial. Astrofiz. Observ.*, 1986.
6. Lawrence, C.R., Bennet, C.L., Hewitt, J.N., Langston, G.I., Klotz, S.E., Burke, B.F., and Turner, K.C., *Astrophys. J., Suppl. Ser.*, 1986, vol. 61, p. 105.
7. Douglas, J.N., *Bull. Am. Astron. Soc.*, 1987, vol. 19, p. 1048.
8. Mingaliev, M.G. and Khabrakhmanov, A.R., *Astron. Zh.*, 1995, vol. 72, p. 12.
9. Verkhodanov, O.V., Trushkin, S.A., Andernach, H., and Chernenkov, V.N., *Astronomical Data Analysis. Software and Systems VI*, ASP Conf. Ser., 1997, vol. 125, p. 322.
10. Nizhel'skii, R.A., *Otchet Spetsial. Astrofiz. Observ.*, 1996, p. 57.
11. Berlin, A.B., Maksyasheva, A.A., Nizhel'skii, N.A., *et al.*, *Tez. Dokl. XXVII Radioastron. Konf.*, St. Peterburg, 1997, vol. 3, p. 115.
12. Gorshkov, A.G. and Khromov, O.I., *Astrofiz. Issled. (Izv. SAO)*, 1981, vol. 14, p. 15.
13. Gorshkov, A.G. and Konnikova, V.K., *Astron. Zh.,* 1996, vol. 73, p. 351.
14. Kuz'min, A.D. and Salomonovich, A.E., *Radioastronomicheskie metody izmereniya parametrov antenn* (Radio Astronomical Methods for Measuring Antenna Parameters), Moscow: Sov. Radio, 1964.
15. Botashev, A.M., Gorshkov, A.G., Konnikova, V.K., and Mingaliev, M.G, *Prep. Spetsial. Astrofiz. Observ.,* 1998, no. 132.
16. Tabara, H. and Inoue, M., *Astron. Astrophys., Suppl. Ser.*, 1980, vol. 39, p. 379.
17. Owen, F., Mintzen, P., and Ulvestad, J., *Astron. J.,* 1983, vol. 88, p. 709.
18. Kellermann, K.I., Mintzen, P., and Ulvestad, J., *Astrophys. J.*, 1971, vol. 169, p. 1.

Translated by G. Rudnitskii